Journal of NeuroVirology (1999) 4, 217–231

http://www.jneurovirol.com

Motor evoked potentials in a rhesus macaque model of neuro-AIDS

Leigh AM Raymond[1,2], Dennis Wallace[2], Joanne K Marcario[1,2], Ravi Raghavan[3], Opendra Narayan[2,3], Larry L Foresman[4], Nancy EJ Berman[2,5] and Paul D Cheney*[,1,2]

[1]Department of Molecular & Integrative Physiology, University of Kansas Medical Center, 3901 Rainbow Blvd., Kansas City, Kansas, KS 66160, USA; [2]Smith Mental Retardation and Human Development Research Center, University of Kansas Medical Center, 3901 Rainbow Blvd., Kansas City, Kansas, KS 66160, USA; [3]Marion Merrell Dow Laboratory for Viral Pathogenesis, University of Kansas Medical Center, 3901 Rainbow Blvd., Kansas City, Kansas, KS 66160, USA; [4]Laboratory Animal Resources, University of Kansas Medical Center, 3901 Rainbow Blvd., Kansas City, Kansas, KS 66160, USA; [5]Anatomy and Cell Biology, University of Kansas Medical Center, 3901 Rainbow Blvd., Kansas City, Kansas, KS 66160, USA

Previous work using bone marrow passaged $SIV_{mac}239$ (simian immunodeficiency virus) has shown that macrophage tropic strains of this virus enter the rhesus macaque brain early following inoculation (Sharma *et al*, 1992; Desrosiers *et al*, 1991; Zhu *et al*, 1995; and Narayan *et al*, 1997). As part of an effort to more fully characterize the extent of neurologic impairment associated with SIV infection of the brain, we used transcranial electrical stimulation of motor cortex and the spinal cord to evoke EMG potentials in two forelimb (EDC and APB) and two hindlimb (LG and AH) muscles. The latencies, magnitudes and thresholds of motor evoked potentials (MEPs) recorded from nine monkeys infected with neurovirulent SIV_{mac} R71/17E were compared to pre-inoculation records from the same monkeys. Seven of nine monkeys developed simian AIDS within 4 months of inoculation and were euthanized. Two monkeys remained free of AIDS-related clinical illness for over 18 months following inoculation. Six of the seven monkeys with rapidly progressing disease showed post-inoculation latency increases ($\geqslant$2 s.d. of control) in at least one cortical MEP. Increases in cortical MEP latency ranged from 21–97% in different monkeys. All seven rapidly progressing animals showed post-inoculation increases in at least one spinal cord MEP latency. Maximum spinal cord MEP latency increases ranged from 22–147%. Increases in central conduction time (CCT) ranged up to 204% and exceeded two standard deviations of control in four monkeys. Neither of the two monkeys with slowly progressing disease showed significant increases in either cortical or spinal cord MEP latency or CCT. Only the monkeys with rapidly progressing disease exhibited classic AIDS-related neuropathology, although there was no consistent relationship between the severity of neuropathology and the extent of MEP abnormalities. In conclusion, our results demonstrate clear deficits in the functional integrity of both central and peripheral motor system structures associated with SIV infection and further support the use of SIV-infected rhesus macaques as a model of neuro-AIDS.

Keywords: monkey; SIV; HIV; AIDS; MEPs; motor deficits; nervous system

Introduction

Neurological complications are a common finding in patients with symptomatic HIV-1 (human immunodeficiency virus) infection. About 10% of AIDS patients first present with a neurological complaint (Janssen, 1997). HIV-1 associated dementia occurs in approximately 20% of patients and is characterized by (1) cognitive impairment including mental slowness, forgetfulness and poor concentration; (2) behavioral changes including apathy, lethargy as well as diminished, dysphoric or inappropriate emotional responses; and (3) motor symptoms including the loss of fine motor control,

*Correspondence: PD Cheney, Smith Mental Retardation Research Center, University of Kansas Medical Center, 3901 Rainbow Boulevard, Kansas City, KS 66160, USA
Received 9 July 1998; revised 21 December 1998; accepted 25 January 1999

unsteady gait and tremor (Navia *et al*, 1986a,b; Navia and Price, 1987; Saykin *et al*, 1991; Glass and Johnson, 1996; Dal Pan *et al*, 1997).

It has been known for many years that HIV-1 enters the central nervous system (CNS) early following exposure (Michaels *et al*, 1988; Sharer, 1992; Epstein and Gendelman, 1993). Once within the CNS, HIV-1 preferentially infects microglia (CNS resident macrophages), although virus has also been isolated from astrocytes (Takahashi *et al*, 1996). Primary infection of neurons has not been convincingly demonstrated (Glass and Johnson, 1996). Neuronal loss associated with HIV-1 infection of the CNS, therefore, has been attributed to secondary processes (Everall *et al*, 1993, 1994; Glass and Johnson, 1996), although some dispute the occurrence of neuron loss (Seilhean *et al*, 1993). Increasing evidence points to several potential neurotoxic factors including cytokines, chemokines, excess neurotransmitters and reactive oxygen species that may be released by HIV-1 infected macrophages or astrocytes and may trigger an excitotoxic cascade (Lipton, 1997).

Motor system deficits are a common component of HIV-1 related cognitive/motor disorder and AIDS-related dementia (Glass and Johnson, 1996; Dal Pan *et al*, 1997). Motor evoked potentials (MEPs) have been used to investigate the integrity of both peripheral and central motor pathways in a number of human disease conditions including HIV-1 infection (Arendt *et al*, 1992; Moglia *et al*, 1991; Connolly *et al*, 1995). MEPs are electromyographic (EMG) potentials recorded from muscles in response to either electrical or magnetic stimulation of the cerebral motor cortex or the spinal cord. Stimulation of motor cortex provides a measure of conduction time along both central corticospinal pathways to spinal cord motoneurons and peripheral conduction from the spinal cord to muscles. Hence, cortical motor evoked potentials provide a measure of total conduction time. Stimulating the spinal cord, on the other hand, provides a measure of conduction time along just the peripheral part of the pathway. A measure of central conduction time can be obtained by subtracting spinal cord MEP latency from cortical MEP latency. Based on a study of 138 HIV-infected patients, Moglia *et al* (1991) reported significant increases in central conduction time in 44% of asymptomatic HIV positive patients and 72% of patients with AIDS. Several studies have also reported slowing in peripheral motor conduction time in both asymptomatic and symptomatic HIV-infected patients (Cornblath and McArthur, 1988; Jakobsen *et al*, 1989; Fuller *et al*, 1991), although the presence and extent of MEP abnormalities in HIV-infected, asymptomatic individuals has been disputed (McAllister *et al*, 1992).

Animal models offer important advantages for the study of retroviral neuropathogenesis. By passaging $SIV_{mac}239$ through bone marrow, Narayan and colleagues developed highly neurovirulent strains of macrophage-tropic SIV_{mac} (Sharma *et al*, 1992; Narayan *et al*, 1997). As in HIV-1 disease, SIV is known to enter the brain early following inoculation and cause productive infection of microglia, and possibly astrocytes, but not neurons (Narayan *et al*, 1997). As in HIV-1 disease, neuronal loss has also been reported in SIV-infected macaques, both in the brainstem and in the cortex (Berman *et al*, 1998; Adamson *et al*, 1996; Weihe *et al*, 1993).

Prospero-Garcia *et al* (1996) demonstrated neurophysiological alterations in cortical and brainstem responses to visual and auditory stimuli in rhesus macaques infected with microglial-passaged $SIV_{mac}251$. More recently, Raymond *et al* (1998) reported delays in the latencies of peaks in the auditory brainstem response of SIV-infected macaques.

Behavioral performance in SIV-infected monkeys has also been examined. Murray *et al* (1992) first demonstrated cognitive and motor impairments in SIV-infected rhesus monkeys using the Delta B670 strain of SIV. Although cognitive deficits were observed in some monkeys on delayed match to sample and visual discrimination and learning tests, nearly all of the monkeys tested (8/10) were impaired on a test of motor skill requiring the monkey to retrieve a food pellet from a rotating disk. More recently, Fox *et al* (1997) reported that rhesus macaques infected with microglial-associated SIV showed deficits in attention set shifting, bimanual motor skill and progressive ratio task performance. We have found that monkeys infected with the same neurovirulent strains of SIV used in the present study showed clear deficits in reaction time and movement time on simple and choice reaction time tasks (Marcario *et al*, 1999). However, decision making time (choice minus simple reaction time) was not consistently affected. Taken together, these studies suggest that while deficits in cognitive function occur in association with SIV disease progression, motor system dysfunction may be more prominent.

Previous studies in both HIV-1 infected humans and SIV-infected monkeys have demonstrated neuronal loss in motor cortex suggesting that the corticospinal system is a target of damage (Masliah *et al*, 1992; Everall *et al*, 1993; Weihe *et al*, 1993). Therefore, the purpose of this study was to test the functional integrity of the forelimb and hindlimb motor output apparatus in rhesus macaques inoculated with a combination of two neurovirulent strains of SIV_{mac}. Our findings show significant slowing in spinal cord (peripheral conduction time) and cortical motor evoked potentials (MEPs) in monkeys with rapidly progressing disease, occurring in as little as 6 weeks following inoculation. Subtracting spinal cord MEP latency from cortical MEP latency revealed that central conduction time was also increased in four of seven monkeys with rapidly progressing disease. Neither of two mon-

keys with slowly progressing disease showed increases in peripheral or central conduction time. Demonstration of SIV-induced motor system pathophysiology confirms the appropriateness of this model for further investigations of the mechanism of AIDS-related neurological impairment.

Results

Mortality and morbidity

A total of nine Rhesus macaques were inoculated with SIV_{mac}R71/17E via femoral bone marrow injection at two different time-points. Four of the nine animals served initially as controls, but after 6 months these monkeys were also inoculated to increase sample size. Seven of nine monkeys progressed to end-stage AIDS within 16 weeks of inoculation and were considered rapid progressors. At necropsy, monkeys exhibited one or more of the following clinical signs: weight loss, diarrhea, tremor, ataxia, weakness, dermatitis, gingivitis, oral lesions, skin lesions, and dysphagia (Table 1). One animal (AQ69) died prematurely from anesthesia associated with a MRI. At the time of death, this monkey had mild weakness and weight loss. Two animals became productively infected with SIV but survived for 109 (AQ15) and 87 weeks (AQ94) weeks and were considered slow progressors. At the time of euthanasia, one of these monkeys (AQ15) exhibited widely disseminated skin tumors, mild wasting and anemia, possibly due to persistent epistaxis; the other monkey (AQ94) was jaundice and showed signs consistent with acute liver disease.

Reproducibility of MEPs

Figure 1 shows examples of single trial EMG responses from two muscles elicited by electrically stimulating the motor cortex (cortical MEPs) and spinal cord (cervical cord MEPs) at different intensities (1.25, 1.5 or 3.0 times threshold for a motor response). Averages of the single trials shown in each column are given in the bottom row of the figure. All measurements were made from averaged records. The somewhat greater trial-to-trial variability in cortical MEPs compared to spinal cord MEPs is probably due largely to fluctuations in cortical and motoneuronal excitability. Nevertheless, latency and magnitude variability in both spinal and cortical MEPs were relatively small yielding average records with highly reproducible features.

Cortical MEP latency changes

Of the seven animals that progressed rapidly to end-stage disease, five (AQ70, 12, 43, 38, 47) showed post-inoculation increases in cortical hindlimb MEP latency that exceeded the control mean by more than two standard deviations (Table 2). Increases were present for both the lateral gastrocnemius (LG) and abductor hallucis (AH) muscles. Six of seven monkeys (all except AQ12) showed increases in cortical forelimb MEPs, although only two of these monkeys (AQ47, AQ38) had increases in both extensor digitorum communis (EDC) and abductor pollicis brevis (APB) muscles. Combining forelimb and hindlimb cortical MEPs, one or more latency was increased in all seven monkeys. Four monkeys showed increases in three or more cortical MEPs; two showed increases in all four cortical MEPs.

Figure 2 shows the distribution of latency changes in SIV-infected monkeys obtained during the final MEP session (end-stage AIDS) compared to pre-inoculation latencies. Data for control monkeys are based on MEPs obtained over a comparable

Table 1. Clinical signs of SIV infected monkeys.

Monkey	*Disease progression*	*Inoculated*	*Death*	*Weeks survived*	*Clinical signs at necropsy*
AQ70	Rapid	01/12/96	04/18/96	14	Weight loss, facial and generalized subcutaneous edema, ataxia, skin lesions, loss of appetite, weakness
AQ69	Rapid	01/12/96	03/16/96	9	Weight loss, resting tremor, epistaxis, skin lesions, weakness
AQ43	Rapid	01/12/96	02/23/96	6	Weight loss, diarrhea, cyanosis, severe ataxia, dysphagia, bleeding gums
AQ12	Rapid	01/12/96	04/16/96	14	Weight loss, diarrhea, cyanosis, severe tremor, severe ataxia, weakness
AQ47	Rapid	07/03/96	08/27/96	8	Weight loss, diarrhea, cyanosis, slight tremor, minor ataxia, loss of appetite
AQ38	Rapid	07/03/96	08/23/96	7	Weight loss, diarrhea, tremor, severe ataxia, skin rash, loss of appetite, weakness
AQ20	Rapid	07/03/96	08/26/96	8	Weight loss, diarrhea, cyanosis, ecchymosis, oral lesions
AQ15	Slow	01/12/96	02/10/98	109	Weight loss, cyanosis, dermatitis, diarrhea, edema, epistaxis, oral lesions, skin lesions, tumors
AQ94	Slow	07/03/96	03/04/98	87	Weight loss, cyanosis, jaundice, diarrhea, weakness, loss of appetite

N/A=not available.

Table 2 Summary of MEP latency increases.

					Cortical				Cord			
Monkey	*Disease progression*	*SIV neuro-pathology†*	*SIV p27 (pg/ml)††*	*CD4 (cells/μl)‡*	*EDC*	*APB*	*LG*	*AH*	*Cervical EDC*	*Cervical APB*	*Lumbar LG*	*Lumbar AH*
AQ69	Rapid	N/A	1288	965	*				*			
AQ70	Rapid	Mild	3830	2356	*		*	*	*	*	*	*
AQ12	Rapid	Moderate	4737	658			*	*	*		*	
AQ43	Rapid	Severe	4902	518		*	*	*	*	*	*	*
AQ38	Rapid	Severe	5238	1187	*	*	*	*	*		*	*
AQ47	Rapid	Mild	5645	1540	*	*	*	*	*	*	*	*
AQ20	Rapid	Mild	5688	51	*					*	*	
AQ15	Slow	Mild	225	177								
AQ94	Slow	None	ND†††	119								

N/A=not available, ND=not detectable. †Applies to motor system structures: motor cortex, basal ganglia, cerebral peduncles, long white tracts, and peripheral nerve. *Latency increase $\geqslant 2$ s.d. of the mean. ††SIV serum p27 is a measure of viral load. †††AQ94 had p27 protein levels as high as 332 earlier during the study. ‡The normal range for CD4 cell counts is $1000-2000/\mu$l. Both p27 and CD4 cell counts are based on the final measurement prior to euthanasia.

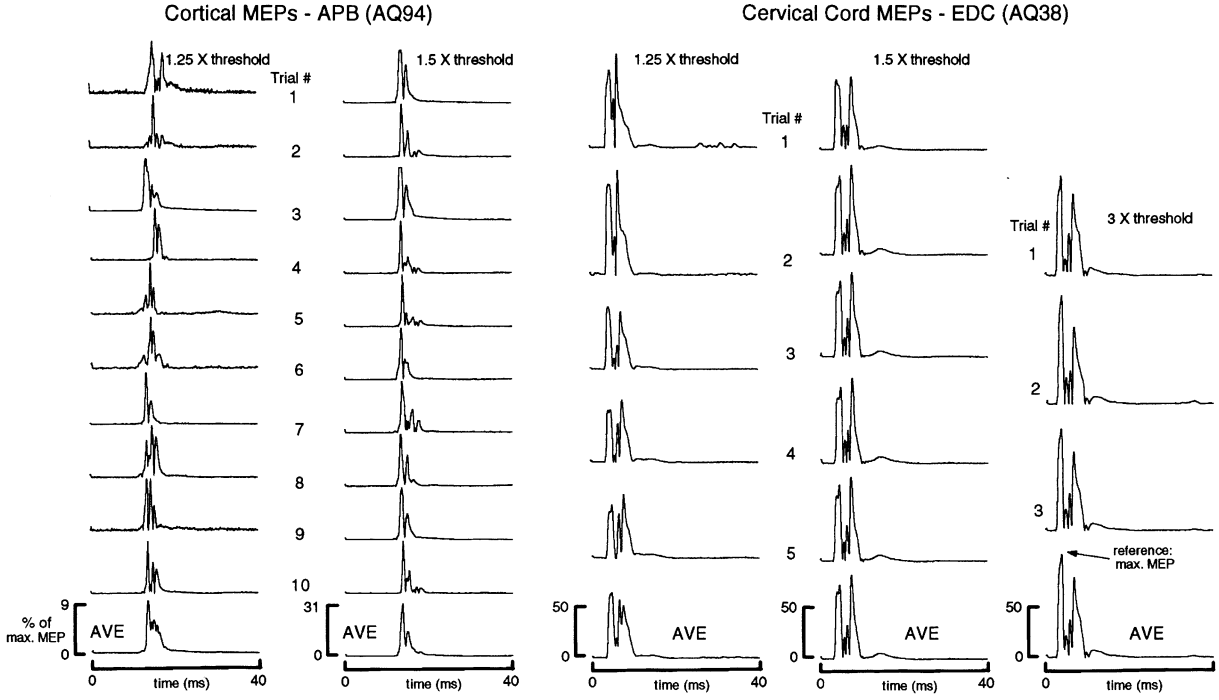

Figure 1 Examples of cortical and cervical cord MEPs illustrating how the data was collected. Ten single trials were collected for cortical MEPs at 1.25 and 1.5 times threshold. For spinal cord MEPs, five single trial records were collected at 1.25 and 1.5 × threshold; two to three were collected at 3 × threshold. The single trial records were then full-wave rectified and averaged. MEP amplitude for the 3 × threshold average record was considered the maximum MEP and assigned a value of 100% for the purpose of quantifying all other records obtained for that muscle.

period of time (6 months). The results presented in this figure differ slightly from the summary in Table 2 because Table 2 takes into account data from all MEP recording sessions. As in Table 2, this figure, depicting changes for the final MEP session, shows that all rapidly progressing monkeys had at least one MEP latency increase that exceeded two standard deviations. None of the latencies of the slowly progressing monkeys exceeded two standard deviations. Maximal increases in cortical MEP latency ranged from 21–97% in different rapidly progressing animals. Changes in cortical MEPs for control monkeys were centered about zero and ranged in magnitude from −7.6 to 7.8%. Reductions in latency (negative changes) observed for SIV monkeys were in the same range as those observed for control monkeys and can be attributed to normal variability. Mean latency increases in LG were

somewhat greater than those in AH (20% *versus* 8%); mean increases in EDC were greater than those in APB (36% *versus* 7%).

Figure 3 shows examples of cortical MEPs from four different monkeys. Records for two rapidly progressing SIV-infected monkeys exhibit clear latency increases while those for a control monkey and a slowly progressing SIV-infected monkey show no changes over a similar period of time.

Spinal cord MEP latency changes

Six of the seven SIV-infected monkeys with rapid progressing disease (all except AQ69) showed post-inoculation increases in spinal cord hindlimb MEP latencies that exceeded the control mean by more than two standard deviations (Table 2). Four of these six showed increases in both hindlimb muscles tested. All seven monkeys showed increases in spinal cord forelimb MEPs, although both EDC and APB latencies were increased in only three of these cases. Neither of the two monkeys with slowly progressing disease showed increases in spinal cord MEP latencies.

Maximum cord MEP latency increases for different rapidly progressing SIV-infected monkeys ranged from 33–147% (Figure 2). Changes for control monkeys were centred about zero and ranged in magnitude from −9.3 to 13.8% for different animals. As with cortical MEPs, latency increases in LG tended to be greater than those in AH (mean increase of 62% *versus* 43%), and EDC appeared to be more strongly affected than APB (mean increase of 25% *versus* 11%).

Figure 4 shows examples of spinal cord MEPs from four different animals. Records for two different rapidly progressing SIV-infected monkeys exhibit clear latency increases while those for a control monkey and a slowly progressing SIV-infected monkey show no changes over a similar period of time.

Central conduction time (CCT) changes

As illustrated in Figure 5, cortical MEP latency is a measure of total conduction time and represents the sum of peripheral (spinal cord MEP latency) and central conduction time. Total conduction time is the sum of conduction along corticospinal axons to spinal motoneurons, synaptic transmission at the motoneuron, time to bring the motoneurons to firing threshold, peripheral nerve conduction, neuromuscular transmission and conduction along muscle fibers to the recording electrodes (Figure 6). Spinal cord MEP latency is a measure of the peripheral component of this pathway including conduction along peripheral motor axons, neuromuscular transmission, and conduction along muscle fibers to the EMG electrode recording site. CCT is routinely computed by subtracting peripheral conduction time (spinal cord MEP latency) from the corresponding total conduction time (cortical MEP latency).

We calculated CCTs for our SIV-infected monkeys and for data collected from the four animals that initially served as controls. Control data were used to define the two standard deviation boundaries. Changes in CCT were examined by calculating the per cent change in post-inoculation CCT (based on data from the final MEP session) compared to pre-inoculation CCT for each monkey. CCT data for control animals was collected over the same length of time as that for the rapid progressors. Four of the rapid progressors (AQ20, AQ12, AQ38, AQ47) showed 50% or greater increases in CCT, well above the two standard deviation criterion (Figure 7). Some smaller decreases in CCT were also observed, although mechanisms other than increased conduction speed probably explain these changes (see Discussion). The two monkeys with slowly progressing disease did not show changes in CCT that differed significantly from changes observed in control monkeys. Although individual monkeys showed increased CCTs, the mean change in CCT for all SIV-infected monkeys of 13.8±23.9% (s.d.) was not significantly different ($P>0.3$, Mann-Whitney rank sum test) from the increase of 3.15±13.6% (s.d.) observed in control animals.

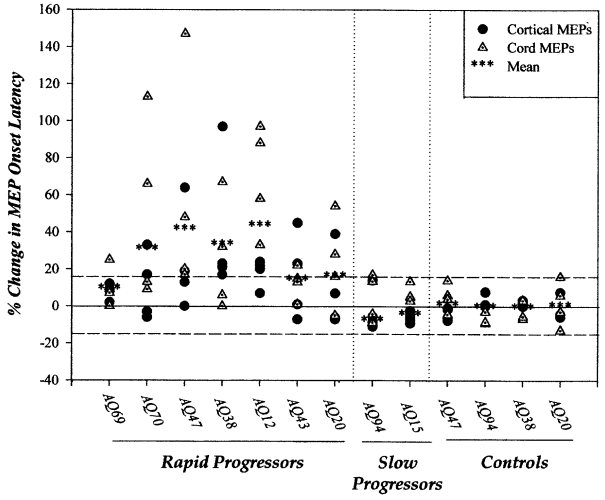

Figure 2 Distribution of cortical and spinal cord MEP latency changes in all nine SIV-infected monkeys and four control monkeys. The dashed lines represent±2 s.d. from the mean of control monkeys. Individual points correspond to MEP latencies for different muscles. Each column contains eight points but in some cases the points are overlapping. Asterisks indicate mean values. Note that the data in this plot differ slightly from Table 2 because this plot is based on the final post-inoculation MEP session whereas the statistical analysis for Table 2 took into account data from all post-inoculation recording sessions. Some of the SIV and control monkey numbers are the same because four monkeys were used over a period of 6 months to collect control data. They were then inoculated to increase the size of the SIV group.

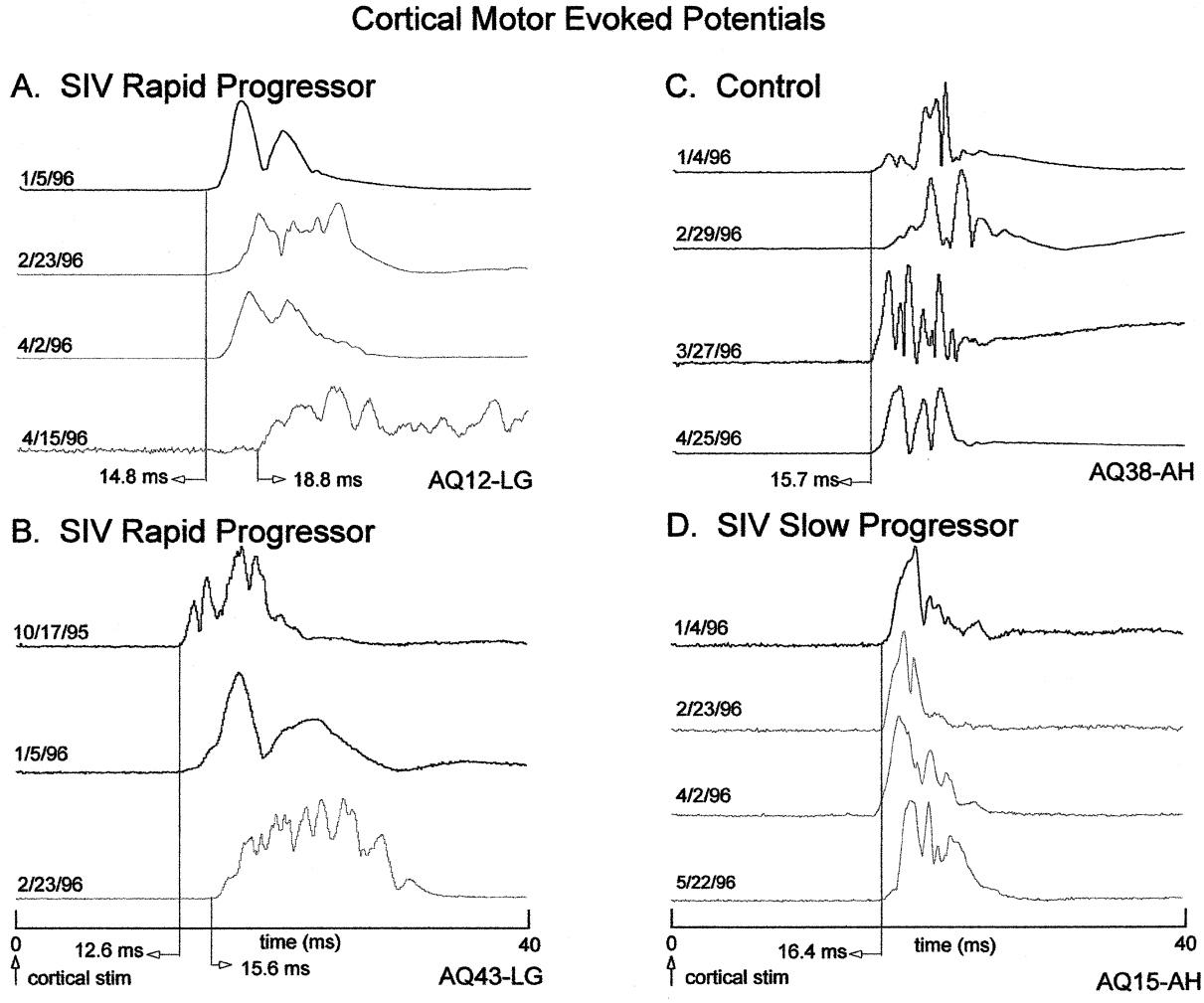

Figure 3 Examples of cortical MEPs recorded over a period of 4–5 months in SIV-infected monkeys and a control monkey. Panels **A** and **B** show records for two SIV-infected monkeys that progressed rapidly to end-stage disease. The last record shown was the final MEP obtained and corresponded with end-stage disease. Panel **C** shows records for an uninoculated control monkey. Panel **D** shows records for a slowly progressing SIV-infected monkey that remained free of clinical signs over the same period of time as data shown for the other monkeys. Cortical MEP latencies did not increase in either the control or slowly progressing monkeys. Light gray records were obtained after the date of inoculation (1/12/96).

Cortical MEP magnitude and threshold changes

Changes in the magnitude of cortical MEPs were expressed as a percentage of maximal ($3\times$ threshold) spinal cord MEP magnitude. Pre-inoculation cortical MEP magnitudes were similar for the forelimb and hindlimb and ranged from 4–60% of maximum in different muscles. Post-inoculation magnitudes ranged from 1–52%. SIV monkeys showed no significant changes in cortical MEP magnitude over a similar time period as that used for control monkeys.

Over the course of the study, we also measured stimulus thresholds for evoking cortical and spinal cord MEPs. Threshold was expressed as a percentage of maximum stimulator output. Pre-inoculation mean thresholds for the SIV-infected monkeys did not differ from the mean thresholds of the last post-inoculation MEP session. Pre-inoculation mean cortical hindlimb and forelimb MEP thresholds were $24\pm7\%$ (s.d.) and $20\pm6\%$ respectively; the corresponding post-inoculation thresholds were 23 ± 5 and $20\pm8\%$. Pre-inoculation mean spinal cord hindlimb and forelimb MEP thresholds were 17 ± 3 and $20\pm4\%$ respectively; the corresponding post-inoculation thresholds were 19 ± 4 and $21\pm7\%$.

Onset of conduction delays in relation to disease progression

In all cases except two, significant MEP conduction delays were only observed for the last evoked potential series when the monkey had reached end-stage disease. Two monkeys (AQ12 and AQ70)

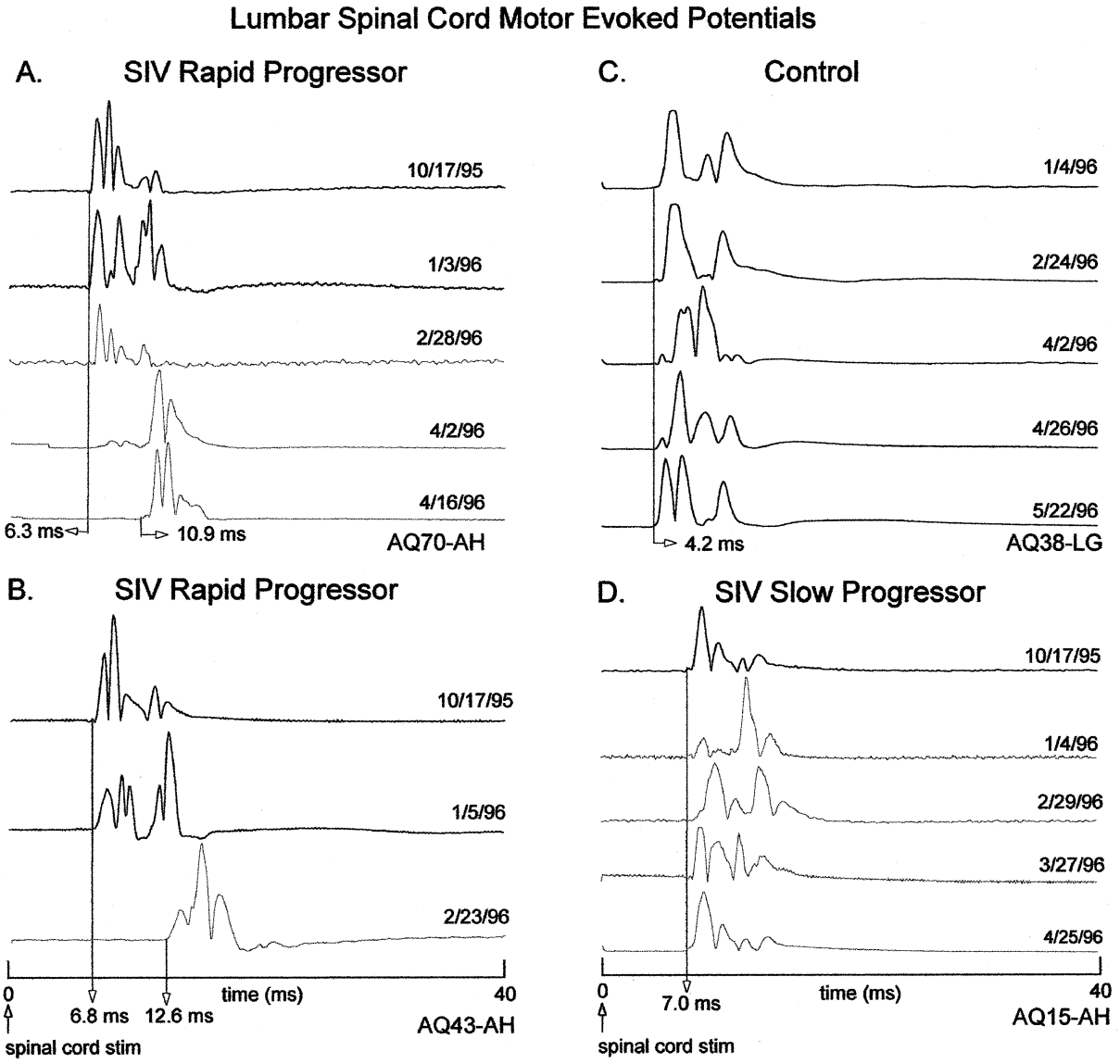

Figure 4 Examples of spinal cord MEPs obtained over a period of 4–6 months in SIV-infected and a control monkeys. Panels **A** and **B** show records for two SIV-infected monkeys that progressed rapidly to end-stage disease. The last record shown was the final MEP obtained and corresponded with end-stage disease. Panel **C** shows records for an uninoculated control monkey. Panel **D** shows records for a slowly progressing SIV-infected monkey that remained free of clinical signs over the same period of time as data shown for the other monkeys. Spinal cord MEP latencies did not increase in either the control or slowly progressing monkeys. All monkeys were infected on 1/12/96. Light gray records were obtained after inoculation.

showed conduction delays in two sessions prior to necropsy providing evidence for progression of neurologic disease. Monkey AQ12 showed progressive increases in cortical and spinal cord hindlimb MEP latency for two sessions prior to necropsy (Figure 3A); monkey AQ70 showed increases in lumbar spinal cord MEPs for two sessions prior to necropsy (Figure 4A). Spinal cord latency changes were observed 2 weeks prior to increases in latency of cortical responses for both AQ12 and AQ70.

Other signs of motor system pathophysiology

Six rapid progressors (all except AQ20) exhibited clinical signs of motor system pathophysiology including ataxia and tremor. One of these monkeys (AQ12) also showed enhanced stretch reflexes and clonus of the ankle extensors (Figure 8). Cortical and spinal cord MEP latency increases were also observed. In fact, this monkey showed one of the largest increases in overall post-inoculation MEP latency (Figure 2).

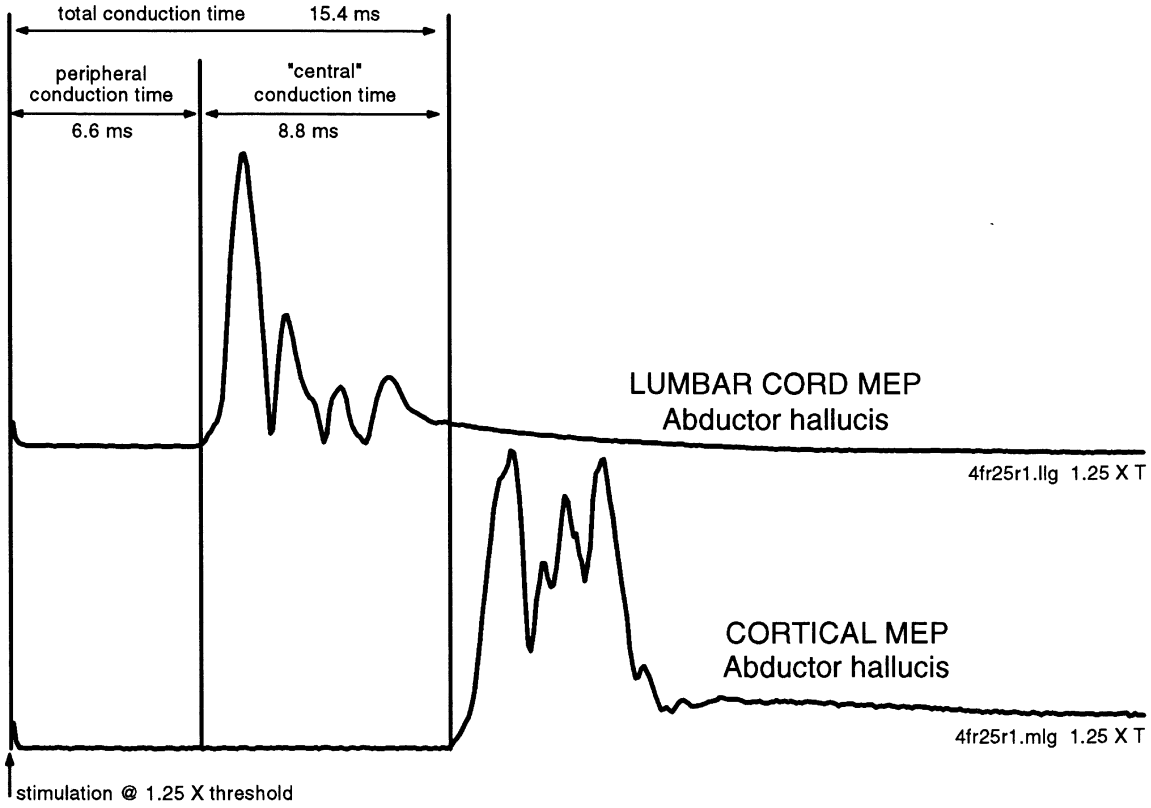

Figure 5 Measurement of MEP latencies. Peripheral conduction time was measured from stimulation of the cervical or lumbar spinal cord. A measure of total conduction time (peripheral and central) was obtained from transcranial electrical stimulation of motor cortex. An estimate of central conduction time (CCT) was obtained by subtracting peripheral conduction time from total conduction time.

Neuropathological, virological and immunological correlations

Evidence of typical retroviral induced CNS neuropathology was observed in seven of eight animals from which tissue was available. Neuropathological findings consisted of perivascular cuffing, microglial nodule formation, multi-nucleate giant cell reactions and peri-lesional axonal degeneration caused by white matter inflammatory lesions. The severity of pathology varied from animal to animal. Macaques AQ43 and AQ38 had severe disseminated meningo-encephalomyelitis in the form of nodular and perivascular mononuclear inflammatory cell infiltrates composed of monocyte-macrophages and microglia, multinucleate giant cells (MGCs) and some lymphocytes (Table 2). In white matter, these infiltrates caused mild perilesional axonal damage and demyelination. Systematic examination of the distribution of lesions along the central and peripheral motor pathways revealed extensive involvement of not only the long tracts (internal capsules, cerebral peduncles, pyramids and descending spinal tracts), but also the grey matter of the motor cortex and deep nuclei. This was accompanied by focal neuronal destruction in the affected areas. In contrast, macaques AQ12, AQ70, AQ47 and AQ20 demonstrated lesions of less intensity and dissemination. Pathology in these animals was restricted to the cerebral white matter and long tracts of the central motor pathways. Grey matter changes or obvious neuronal destruction was not a feature in these animals.

Significant involvement of the spinal anterior horn cells or peripheral nerves was not obvious. At necropsy, samples of peripheral nerve (median, tibial, sciatic and femoral) were routinely taken and examined for evidence of pathology using light microscopy and tissue sections stained with hematoxylin and eosin. Peripheral nerve lesions were rare and seen only in macaque AQ12.

It is noteworthy that all monkeys with rapidly progressing disease, in which a pathological analysis was possible, showed classic AIDS-related neuropathology (microglial nodules and multinucleate giant cells). In contrast, neither of the two animals with slowly progressing disease showed classic AIDS-related neuropathology, even though the post-inoculation life-spans of these monkeys were much longer and they did develop clinical AIDS-related disease. AQ15 showed only mild,

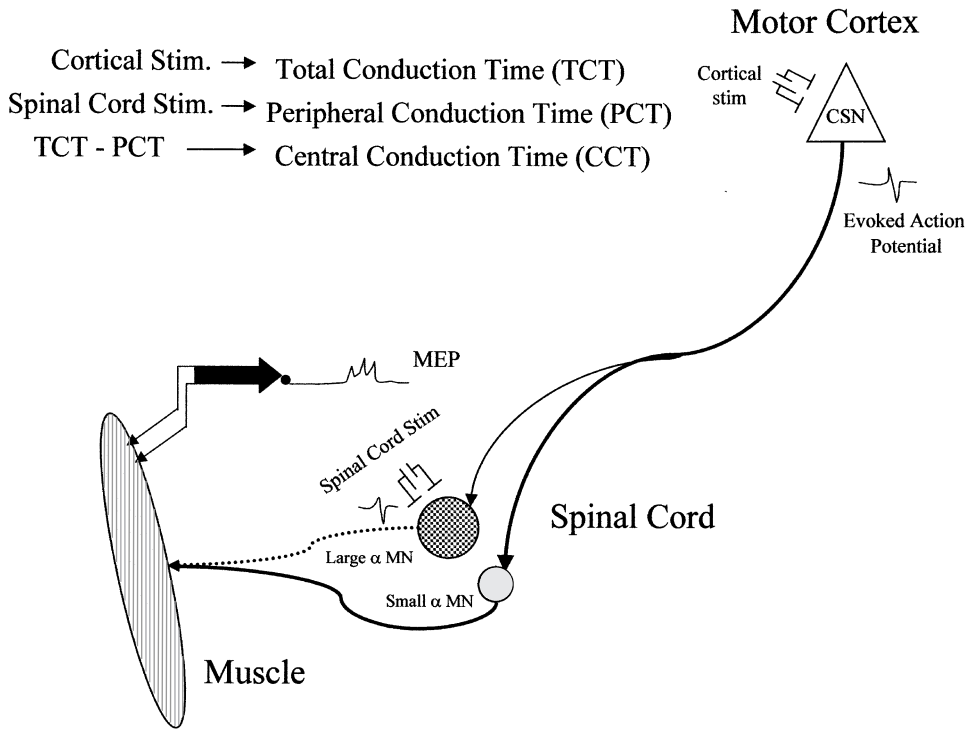

Figure 6 Illustration of the motor output pathways underlying cortical and spinal cord MEPs. Transcranial electrical stimulation evokes a descending volley of action potentials in corticospinal neurons (CSN). Many of these neurons make monosynaptic excitatory connections with large and small alpha motoneurons. However, at the relatively low intensities of stimulation used in this study, cortical MEPs will primarily reflect activation of the smaller motoneurons due to the principle of orderly recruitment according to size. In contrast, because electrical stimulation activates large axons at lower stimulus intensities then small axons, our spinal cord MEPs will primarily reflect activation of large motor axons. This has important implications for interpreting central conduction time data.

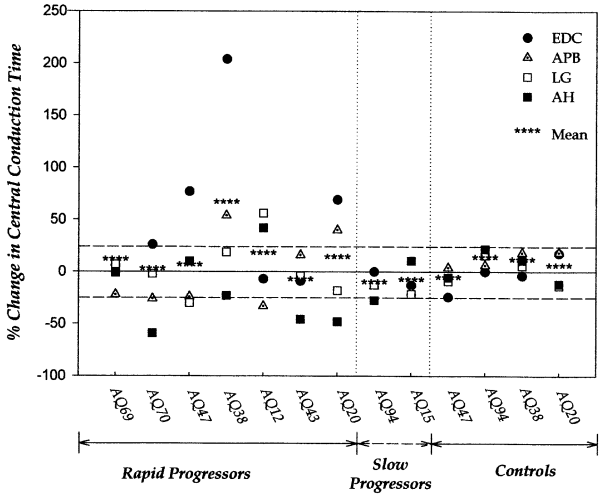

Figure 7 Distribution of central conduction time (CCT) changes for all nine SIV-infected monkeys and four monkeys that initially served as control animals. The dashed lines represent ± 2 s.d. from the mean of the control data. Individual points illustrate CCT for different muscles. Each column contains four points but in some cases the points are overlapping. This plot is based on the per cent difference between the pre-inoculation and final post-inoculation CCTs for each animal and muscle. Control data was collected over a period of 6 months and the per cent difference between the first and last control sessions are shown.

focal meningo-encephalitis and AQ94 had no neuropathological changes involving motor system structures. However, it should be noted that the severity of motor system neuropathology did not always match the extent of MEP abnormalities. For example, AQ47 and AQ70 had only mild neuropathological changes, but both of these monkeys showed marked changes in nearly all MEPs tested (Table 2, Figure 2).

Neither was there a consistent relationship between viral load (p27 levels) or CD4 cell count and the extent of MEP abnormalities within the group of rapid progressors (Table 2, Figure 2). However, the fact that the slow progressors showed no MEP deficits and had very low viral loads and also low CD4 cell counts compared to the rapid progressors suggests that viral load is a more important predictor of neurological injury.

Discussion

In this study we present evidence for delays in cortical and spinal cord MEPs associated with neurovirulent SIV infection in rhesus macaques. Of nine infected monkeys on which data was

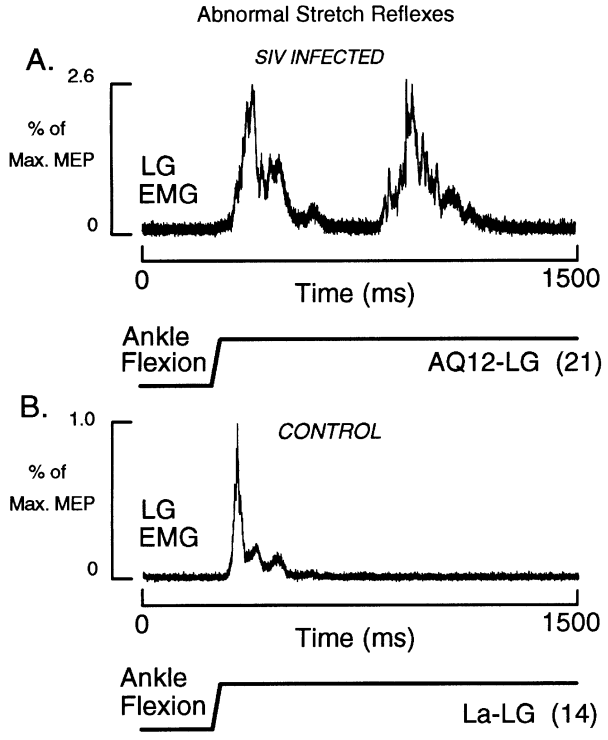

Figure 8 Abnormal stretch reflex response obtained from the lateral gastrocnemius in one SIV-infected monkey (AQ12) that exhibited clinical neurological symptoms including ataxia and tremor. Rapid ankle flexion denoted by the lower record produced a reflex response that was larger and prolonged compared to that obtained from a control monkey (**B**) under similar conditions. Even more abnormal was the existence of a second, equally large reflex response suggesting the presence of clonus. Average records based on 21 trials in **A** and 14 trials in **B**. Magnitude was quantified in relation to the 3 × threshold lumbar cord MEP taken as 100%. Note the difference in vertical scales.

collected, seven progressed to end-stage disease within a period of 4 months or less (rapid progressors) and all of these monkeys showed latency increases in at least one of eight MEP types (cortical and spinal cord MEPs for each of four muscles). In some cases, latency increases were present over multiple post-inoculation test sessions. However, the magnitude of latency increases were most prominent for the last recording session corresponding to end-stage disease.

In two monkeys (AQ15 and AQ94) disease progression was slow. At 87 and 109 weeks respectively, complications related to systemic disease (wasting, liver dysfunction and skin tumors) necessitated euthanasia. At necropsy, these two animals had p27 levels that were much lower than monkeys with rapidly progressing disease (Table 2). In fact, blood levels of p27 remained low (<60 pg/ml) over most of the disease course. CD4+ cells showed a progressive decline over a period of several months and at the time of necropsy were lower than most of the monkeys with rapidly progressing disease. Neither AQ15 nor AQ94 showed significant MEP latency increases. Neither did these two monkeys show increases in the latency of auditory brainstem responses (Raymond *et al*, 1998). Based on these findings and the complimentary findings of Westmoreland *et al* (1998), we conclude that these two monkeys developed systemic AIDS in the absence of significant neurological disease and that SIV induced encephalitis and neurologic impairment is characteristic of rapid disease progression.

Spinal cord MEPs provide a measure of peripheral conduction time (Mills and Murray, 1986; Kimura, 1989). Increased peripheral conduction time is most easily attributed to axonal conduction slowing or failure, possibly related to demyelination or axonal loss. Despite the fact that peripheral conduction latencies showed large increases (as much as 147%), peripheral nerve pathology visible at the light microscopic level appeared to be minimal. Only one monkey (AQ12) showed clear evidence of peripheral nerve inflammatory lesions. However, our histological technique could have missed more subtle axonal loss or demyelination. Also, peripheral nerve pathology may have been localized to regions of the nerve that we did not examine. Using simple light microscopy, we examined 2 cm long sections of different peripheral nerves (median, sciatic, posterior tibial, and femoral) in both longitudinal and transverse sections. In the absence of overt structural pathology, conduction slowing could result from a pathophysiological process affecting ion channels and excitability (Koller *et al*, 1997). In any case, the increases in spinal cord MEP latencies indicate the presence of underlying peripheral nerve pathophysiology if not actual neuropathy or myelopathy.

We computed CCT by subtracting spinal cord MEP latency (peripheral conduction time) from the corresponding cortical MEP latency (total conduction time). We observed substantial increases in CCT in four monkeys suggesting slowing of central motor pathways. This is consistent with clear evidence of CNS white matter pathology in our animals. It is of interest that changes in CCT were only observed for animals with rapidly progressing SIV disease. Monkeys with slowly progressing disease did not show changes in either central or peripheral conduction time.

It is puzzling that decreases in CCT time were also observed (Figure 7). The possibility that this might be due to actual increased central conduction velocity seems highly unlikely, but there are other factors that might explain this result. For example, it is likely that cortical and spinal cord MEPs are mediated predominately by small (slowly conducting) and large (rapidly conducting) motoneurons respectively. This is because cortical MEPs involve synaptic activation of motoneurons whereas spinal cord MEPs involve electrical stimulation of motoneuron axons (Kimura, 1989). What is most relevant

for our study is the possibility that viral injury may preferentially affect large axons as suggested by Fuller *et al* (1991). In this case, and given that the cortical and spinal cord MEPs rely on slow and fast conducting motoneurons respectively, marked peripheral MEP latency increases could occur without comparable cortical MEP latency increases (Figure 6). Comparison of pre- and post-inoculation CCTs might then yield negative changes, falsely suggesting faster conduction (Figure 7).

Studies of MEPs in asymptomatic and symptomatic HIV-infected humans have yielded conflicting results. All studies seem to agree that the late stages of disease (CDC stage IV) are characterized by a clear peripheral neuropathy involving both sensory and motor axons (Cornblath and McArthur, 1988), although some even question this (McAllister *et al*, 1992). However, several studies report peripheral conduction slowing associated with earlier, asymptomatic stages of disease (Jakobsen *et al*, 1989; Fuller *et al*, 1991), while others find that peripheral conduction slowing is only present when disease has progressed to a late stage and clinical symptoms are present (Farnarier and Somma Mauvais, 1990; Ronchi *et al*, 1992). Reports of central motor slowing are also conflicting. Moglia *et al* (1991) found slowing of transcranial MEPs in both HIV positive, asymptomatic patients (44%) and patients with AIDS (72%). They attributed most of the slowing to defects in central motor conduction time. Others have also reported prolonged central motor conduction time in asymptomatic, HIV positive patients (Farnarier and Somma Mauvais, 1990; Somma Mauvais and Farnarier, 1992). In contrast, Grapperon *et al* (1993) and Arendt *et al* (1992) found no evidence of conduction defects in central motor pathways in either asymptomatic or symptomatic patients. Our findings support the view that MEP deficits are present, but associated with the later stages of disease progression. These deficits can be attributed to increases in both peripheral and central conduction time.

All our animals became productively infected with SIV_{mac}R71/17E as demonstrated by the substantial levels of p27 found in blood (Table 2). It should be noted that AQ94 had viral p27 protein levels as high as 332 pg/ml at one point during disease progression although in the final sample, p27 was undetectable. Of particular interest is the fact that at the time of necropsy, monkeys with slowly progressing disease had very low levels of virus but also had very low CD4 cell counts compared to monkeys with rapidly progressing disease. Relating this finding to the fact that slowly progressing monkeys did not show MEP deficits, while rapid progressors did, suggests that viral load is a better predictor of neurological injury than CD4 cell count. However, within the group of rapid progressors, neither viral load nor CD4 cell count was a good predictor of the severity of MEP abnormalities.

The severity of classic AIDS-related neuropathology (microglial cells, multi-nucleate giant cells) was also variable. Only the monkeys with rapid progressing disease developed classic AIDS-related neuropathology and only the rapid progressors showed MEP deficits. Therefore, at this level, there was good agreement between neuropathological and MEP findings. However, it should be emphasized that within the group of rapid progressors, the severity of pathology was not a good predictor of the severity of MEP deficits. For example, two monkeys with only mild pathology had extensive MEP abnormalities (AQ47 and AQ70; Table 2). Discordance between pathology and function has also been noted in studies of HIV-1 infected humans (Glass *et al*, 1993; Everall *et al*, 1994) and in a previous study of behavioural deficits in rhesus macaques infected with the Delta B670 strain of SIV (Rausch *et al*, 1994).

In conclusion, we have demonstrated substantial post-inoculation latency increases in both spinal cord and cortical MEPs in SIV_{mac}R71/17E infected rhesus macaques with rapidly progressing disease. Over half of the monkeys with rapidly progressing disease also showed substantial increases in CCT. Therefore, both peripheral and central motor pathways seem to be targets of SIV-related pathophysiology. We attribute delays in peripheral and central conduction to injury of corticospinal neurons and motoneurons, respectively. While demyelination and/or neuronal loss is the most likely explanation of this slowing, the lack of obvious peripheral nerve pathology in most of our monkeys raises the possibility of functional injury (Koller *et al*, 1997). These results further establish the SIV_{mac}R71/17E infected macaque monkey as a useful model of neuro-AIDS, including a possible model for the peripheral myelopathy and neuropathy often associated with HIV-1 infection.

Materials and methods

Subjects

Nine, adolescent, male rhesus macaques of Indian origin were inoculated via bone marrow injection of the femur with SIV_{mac}R71/17E. Each animal received 0.5 ml of each homogenate for a total volume of 1 ml containing approximately 1000 $TCID_{50}$. The monkeys were free of SIV and Herpes B Virus. Four of the monkeys initially served as sex and age matched controls over a period of 6 months during which data were also collected from five monkeys infected with SIV. After 6 months, the four control monkeys were also inoculated to increase the size of the SIV cohort. Daily body temperature and health observations were noted over the course of disease progression (Table 1). Blood and CSF samples were collected from all animals once a week for the first month after inoculation, every 2 weeks for the second month, and thereafter at 4-week intervals. All inoculated monkeys became productively infected with SIV as

demonstrated by blood levels of p27. Seven of the nine infected monkeys exhibited rapidly progressing disease and were euthanized within 4 months of inoculation after developing signs of end-stage simian AIDS. Disease progression was slow in two other monkeys (AQ15 and AQ94). These monkeys were euthanized at 109 and 87 weeks post-inoculation due to systemic complications including wasting, skin tumors and liver disease.

Monkeys were euthanized when one of the following criteria were met: (1) weight loss exceeding 20% of body weight, (2) inability to maintain a sitting posture, (3) failure to eat or drink, or (4) diarrhea unresponsive to treatment. All procedures in this study conformed to the *Guide for the Care and Use of Laboratory Animals* published by the U.S. Department of Health and Human Services, National Institutes of Health. The monkeys in this study were also trained to perform behavioral tasks (reaction time, working memory, and motor skill) that were used to detect cognitive and motor impairments. A battery of sensory evoked potentials were also recorded. Results of the behavioural and sensory evoked potential studies will be the subject of other papers.

MEP recording methods

MEPs were recorded at 4-week intervals including one, or in some cases, two pre-inoculation sessions. Following an initial injection of ketamine (10 mg/kg with atropine at 0.1 mg/kg), anesthesia was maintained by subsequent doses of ketamine (10 mg/kg) every 20–30 min. Body temperature was measured at the start and completion of each EP session using an infrared tympanic thermometer. Temperature was maintained by surrounding the animal with heated saline bottles during recording. Subdermal platinum needle electrodes (Grass™ model E2) were used for differential recording of EMG potentials evoked by transcranial electrical stimulation of the motor cortex. Recordings were made from two hindlimb muscles – lateral gastrocnemius (LG) and abductor hallucis (AH), and two forelimb muscles – extensor digitorum communis (EDC) and abductor pollicis brevis (APB).

MEPs were elicited using a modified bipolar hand held stimulating electrode (Digitimer model DS180-031). The cathode and anode were separated by 4 cm and consisted of 1 cm diameter saline soaked pads. Conductive gel was used to further reduce resistance. Current pulses (50 microsecond duration) were generated by a high voltage stimulator (Digitimer™ Model DS180). MEPS were recorded using Neurolog amplifiers (Digitimer™ NL820 and NL822 preamplifier) with filter settings of 30 Hz – 10 kHz. EMG signals were digitized at 10 KHz and averaged using custom software (Neural Averager, Larry Shupe, University of Washington, Seattle) written for the Windows™ operating system and Cambridge Electronic Design 1401 plus data acquisition hardware. Averaged MEPs were based on ten stimulus repetitions for cortical MEPs and five repetitions for spinal cord MEPs.

Cortical MEPs provide a measure of total motor system conduction time including central and peripheral components. Cortical MEPs were elicited by placing the anode on the scalp overlying either hindlimb motor cortex (near Cz) or forelimb motor cortex (near C3). The cathode was positioned anteriorally on the contralateral side of the skull. MEP thresholds were determined at a gain of 10 K and expressed as a percentage of maximum stimulator output. The lowest threshold position was determined by stimulating at different scalp locations while observing MEPs on an oscilloscope screen. Cortical MEPs were recorded at 1.25 and 1.5 times the threshold of the forelimb or hindlimb muscle with the highest threshold (Figure 1).

Forelimb and hindlimb spinal cord MEPs were determined by positioning the cathode over the cervical and lumbar enlargements respectively. Spinal cord MEPs provided a measure of peripheral motor system functional integrity. Cord MEPs were recorded at 1.25, 1.5 and $3 \times$ threshold. Averages were based on either five trials (1.25 and $1.5 \times$ T) or two to three trials ($3 \times$ T condition). The axis of the electrode was aligned with the axis of the vertebral column. The cathode was located caudally. This method of spinal cord stimulation most likely excites motor axons directly at the level of the axon hillock (Mills and Murray, 1986; Kimura, 1989).

Measurement and analysis of MEPs

Single trial MEP records were full-wave rectified and averaged (Figure 1). Rectification avoids potential cancellation of components in raw EMG signals that could affect magnitude measurements. MEP onset latency was computer measured from averaged records. Cord MEP onset latency provides a measure of peripheral conduction time while cortical MEP latency provides a measure total conduction time. As illustrated in Figure 5, we also obtained a measure of central conduction time (CCT) by subtracting spinal cord MEP latency from cortical MEP latency. Cortical MEP magnitude was quantified by expressing the peak and area as a percentage of the maximal cord MEP obtained at $3 \times$ threshold. Cortical MEPs were generally about 15% the magnitude of maximal cord MEPs.

Statistical analysis

Quantitation of baseline variability in spinal cord and cortical MEPs was based on data collected from four monkeys that served as controls over a period of 6 months. The significance of post-inoculation changes in MEP latency, magnitude and threshold was interpreted in relation to the standard deviation of data from control monkeys. Post-inoculation MEP latencies, magnitudes and thresholds that exceeded two standard deviations of control values

were judged to be significant. The statistical analyses were designed to provide descriptions of the relationship between SIV infection and MEP outcomes and are considered exploratory rather than inferential. Both single subject and population analyses were performed. MEP latencies for individual animals were examined graphically using procedures analogous to Shewert control charts often used in industrial process control (Box *et al*, 1978). To generate estimates of within monkey variability needed to construct the control charts, a variance components analysis was applied to the pre-inoculation observations from all nine monkeys to partition MEP latency variability into between-animal and within-animal components. Control charts for each animal were then constructed using the mean pre-inoculation latency for that animal and the average within-monkey standard deviation obtained from the variance components analysis. Plots of the post-inoculation latencies were then compared to the expected range (mean ± 2 standard deviations) to assess whether SIV infection was indicative of MEP pathophysiology. Separate analyses were conducted for each MEP type (source and muscle) for the 1.25 threshold condition.

Histology and neuropathology

At necropsy, monkeys were given an initial dose of ketamine (10 mg/kg) followed by a near lethal, I.V. dose of pentobarbital. All animals (except AQ47 and AQ43) were exsanguinated through the descending aorta and perfused transcardially with two liters of normal saline followed by two liters of 10% neutral buffered formalin. AQ47 and AQ43 were not perfused with formalin so that fresh tissue samples could be taken for molecular analysis. Following fixation either by perfusion, or in the case of AQ47 and AQ43 immersion, the brain, spinal cord and some peripheral nerves (median, tibial, sciatic and femoral) were removed and processed for histopathological analysis.

From an earlier constructed dissection map of the typical macaque brain, the right hemispheres were dissected at 10 mm intervals in the coronal plane providing access to the following regions of the motor pathway: the motor and pre-motor cortices, the basal ganglia (including the caudate, putamen and globus pallidus), thalamus and the deep white matter (including the internal and external capsules, comissural fibers and the periventricular white matter). The brainstem was dissected transversely at 5 mm intervals and samples included the upper and lower mid-brain at the levels of the superior and inferior colliculi, the mid-pons and the upper and lower medulla (including the pyramids and lower cranial nerves). The spinal cord was sectioned transversely at 10 mm intervals through the cervical (C2 and C7/C8), thoracic (T2, T6 and T10) and lumbar (L2 and L5) segments. After embedding the tissue in paraffin, 5 μm serial sections were stained with hematoxylin and eosin (H&E), Luxol Fast Blue and Sevier Munger stains to assess suspected neuropathology. The severity of motor system pathology was scored in a semi-quantitative fashion based on the number, size and type of lesions per microscopic field.

Two centimeter long segments of the median, sciatic, posterior tibial and femoral (AQ43 only) nerves were removed, embedded in paraffin and sectioned first transversely and then longitudinally at 5 μm. Three to six transverse sections and three serial longitudinal sections were examined for each nerve. The sections were mounted on gelatin coated slides, stained with H and E, and examined for evidence of axonal loss and/or demyelination using light microscopy. A complete report of the neuropathology is available elsewhere (Ragahavan *et al*, 1999).

Acknowledgements

The authors thank Randall Lininger and Jill Brandom-Harris for their expert technical contributions. In addition, we thank Jim Rengel and Ted Gleason for assistance with electronics, Drs David Pinson and Istavan Adany, for their assistance with the necropsies and tissue cataloging and Dr Richard Dubinsky for help in evaluating neurological symptoms. This research was supported by NIH grants NS32203 and HD02528.

References

Adamson DC, Dawson TM, Zink MC, Clements JE, Dawson VL (1996). Neurovirulent simian immunodeficiency virus infection induces neuronal, endothelial and glial apoptosis. *Mol Medicine* **2:** 417–428.

Arendt G, Maecker HP, Jablonowski H, Hombert V (1992). Magnetic stimulation of motor cortex in relation to fastest voluntary motor activity in neurologically asymptomatic HIV-positive patients. *J Neurol Sci* **112:** 76–80.

Berman NEJ, Raymond LA, Warren KA, Raghavan R, Joag SV, Narayan O, Cheney PD (1998). Fractionator analysis shows loss of neurons in the lateral geniculate nucleus of macaques infected with neurovirulent simian immunodeficiency virus. *Neuropathol Appl Neurobiol* **24:** 44–52.

Box GEP, Hunter WG, Hunter JS (1978). *Statistics for Experimenters.* Wiley and Sons: New York, pp 556–563.

Connolly S, Manji H, McAllister RH, Griffin GB, Loveday C, Kirkis C, Sweeney B, Sartawi O, Durrance P, Fell M, Boland M, Fowler CJ, Newman SP, Weller IVD, Harrison MJG (1995). Neurophysiological assessment of peripheral nerve and spinal cord function in asymptomatic HIV-1 infection: results from the UCMSM/Medical Research Council neurology cohort. *J Neurol* **242:** 406–414.

Cornblath DR, McArthur JC (1988). Predominantly sensory neuropathy in patients with AIDS and AIDS-related complex. *Neurology* **38:** 794–796.

Dal Pan GJ, McArthur JC, Harrison MJG (1997). Neurological symptoms in human immunodeficiency virus infection. In: *AIDS and the Nervous System.* Berger JR, Levy RM, (eds). Lippincott-Raven: Philadelphia, pp 141–172.

Desrosiers RC, Hansen-Moosa A, Mori K, Bouvier DP, King NW, Daniel MD, Ringler DJ (1991). Macrophage-tropic variants of SIV are associated with specific AIDS related lesions but are not essential for the development of AIDs. *Amer J Pathol* **139:** 29–35.

Epstein LG, Gendelman HE (1993). Human immunodeficiency virus type 1 infection of the nervous system: pathogenetic mechanisms. *Ann Neurol* **33:** 429–436.

Everall IP, Luthert P, Lantos P (1993). A review of neuronal damage in human immunodeficiency virus infection: its assessment, possible mechanism and relationship to dementia. *J Neuropathol Exp Neurol* **52:** 561–566.

Everall IP, Glass JD, McArthur J, Spargo E, Lantos P (1994). Neuronal density in the superior frontal and temporal gyri does not correlate with the degree of human immunodeficiency virus-associated dementia. *Acta Neuropathol* **88:** 538–544.

Farnarier G, Somma Mauvais H (1990). Multimodal evoked potentials in HIV infected patients. *Electroenceph Clin Neurophysiol* **41,** 355–369.

Fox HS, Gold LH, Henriksen SJ, Bloom FE (1997). Simian immunodeficiency virus: a model for neuro-AIDS. *Neurobiol Disease* **4:** 265–274.

Fuller GN, Jacobs JM, Guiloff RJ (1991). Subclinical peripheral nerve involvement in AIDS: an electrophysiological and pathological study. *J Neurol Neurosurg Psychiatry* **54:** 318–324.

Glass JD, Johnson RT (1996). Human immunodeficiency virus and the brain. *Ann Rev Neurosci* **19:** 1–26.

Glass JD, Wesselingh SL, Selnes OA, McArthur JC (1993). Clinical-neuropathologic correlation in HIV-associated dementia. *Neurology* **43:** 2230–2237.

Grapperon J, Trousset A, Jaubert D (1993). Central and peripheral nervous system motor conduction rate in HIV infection. *Presse Med* **22:** 1302–1306.

Jakobsen J, Smith T, Gaub J, Helweg Larsen S, Trojaborg W (1989). Progressive neurological dysfunction during latent HIV infection. *British Med J* **299,** 225–228.

Janssen RS (1997). Epidemiology and neuroepidemiology of human immunodeficiency virus infection. In: *AIDS and the Nervous System.* Berger JR, Levy RM (eds). Lippincott-Raven: Philadelphia, pp 13–37.

Koller H, Siebler M, Hartung HP (1997). Immunologically induced electrophysiological dysfunction: implications for inflammatory diseases of the CNS and PNS. *Prog Neurobiol* **52:** 1–26.

Kimura J (1989). *Electrodiagnosis in Diseases of Nerve and Muscle: Principles and Practice.* F. A. Davis Co.: Philadelphia.

Lipton SA (1997). Treating AIDS dementia. *Science* **276:** 1629–1630.

Marcario JK, Raymond LAM, McKiernan BJ, Foresman LL, Joag SV, Raghavan R, Narayan O, Hershberger S, Cheney PD (1999). Simple and choice reaction time performance in SIV-infected Rhesus macaques. *AIDS Res Hum Retroviruses* **15:** 571–584.

Masliah E, Ge N, Achim CL, Hansen LA, Wiley CA (1992). Selective neuronal vulnerability in HIV encephalitis. *J Neuropath Exp Neurol* **51:** 585–593.

McAllister RH, Herns MV, Harrison MJ, Newman SP, Connolly S, Fowler CJ, Fell M, Durrance P, Manji H, Kendall BE, Valentine AR, Weller IVD, Adler M (1992). Neurological and neuropsychological performance in HIV seropositive men without symptoms. *J Neurol Neurosurg Psychiatry* **55:** 143–148.

Michaels J, Sharer LR, Epstein LG (1988). Human immunodeficiency virus type 1 (HIV-1) infection of the nervous system: a review. *Immunodefic Rev* **1:** 71–104.

Mills KR, Murray NMF (1986). Electrical stimulation over the human vertebral column: which neural elements are excited? *Electroenceph Clin Neurophysiol* **63:** 582–589.

Moglia A, Zandrini C, Alfonsi E, Rondanelli EG, Bono G, Nappi G (1991). Neurophysiological markers of central and peripheral involvement of the nervous system in HIV-infection. *Clin Electroencephalography* **22:** 193–198.

Murray EA, Rausch DM, Lendvay J, Sharer LR, Eiden LE (1992). Cognitive and motor impairments associated with SIV infection in rhesus monkeys. *Science* **255:** 1246–1249.

Narayan O, Raghavan R, Stephens EB, Joag SV (1997). Animal models of human immunodeficiency virus neurological disease. In: *AIDS and the Nervous System.* Berger JR, Levy RM (eds). Lippincott-Raven Publishers: Philadelphia.

Navia BA, Cho ES, Petito CK, Price RW (1986a). The AIDS dementia complex: II. Neuropathology. *Ann Neurol* **19:** 525–535.

Navia BA, Jordan BD, Price RW. (1986b). The AIDS dementia complex: I. Clinical features. *Ann Neurol* **19:** 517–524.

Navia BA, Price RW (1987). The acquired immunodeficiency syndrome dementia complex as the presenting or sole manifestation of human immunodeficiency virus infection. *Arch Neurol* **44:** 65–69.

Prospéro-García O, Gold LH, Fox HS, Polis I, Koob GF, Bloom FE, Henriksen SJ (1996). Microglia passaged simian immunodeficiency virus induces neurophysiological abnormalities in monkeys. *Proc Natl Acad Sci USA* **93:** 14158–14163.

Raghavan R, Cheney PD, Raymond LA, Joag SJ, Stephens EB, Adany I, Pinson DM, Zhuang L, Marcario JK, Jia F, Wang C, Foresman L, Berman NEJ, Narayan O (1999). Morphological correlates of neurological dyhsfunction in macaques infected with neurovirulent simian immunodeficiency virus. *Neuropath Appl Neurobiol:* in press.

Rausch DM, Heyes MP, Murray EA, Lendvay J, Sharer LR, Ward JM, Rhem S, Nohr D, Weihe E, Eiden LE (1994). Cytopathological and neurochemical correlates of progression to motor/cognitive impairment in SIV-infected rhesus monkeys. *J Neuropathol Exp Neurol* **53:** 165–175.

Raymond LAM, Wallace D, Berman NEJ, Marcario J, Foresman L, Joag SV, Ragahavan R, Narayan O, Cheney PD (1988). Auditory brainstem responses in a Rhesus macaque model of neuro-AIDS. *J Neuro Virol* **4:** 512–520.

Ronchi O, Grippo A, Ghidini P, Lolli F, Lorenzo M, Di Pietro M, Mazzotta F (1992). Electrophysiologic study of HIV-1 + patients without signs of peripheral neuropathy. *J Neurol Sci* **113:** 209–213.

Saykin AJ, Janssen RS, Sprehn GC, Kaplan JE, Spira TJ, O'Connor B (1991). Longitudinal evaluation of neuropsyhchological function in homosexual men with HIV infection: 18-month follow-up. *J Neuropsychiatry Clin Neurosci* **3,** 286–298.

Seilhean D, Duyckaerts C, Vazeux R, Bolgert F, Brunet P, Katlama C, Gentilini M, Hauw JJ (1993). HIV-1-associated cognitive/motor complex: absence of neuronal loss in the cerebral neocortex. *Neurology* **43:** 1492–1499.

Sharer LR (1992). Pathology of HIV-1 infection of the central nervous system. A review. *J Neuropathol Exp Neurol* **51:** 3–11.

Sharma DP, Zink MC, Anderson M, Adams R, Clements JE, Joag SV, Narayan O (1992). Derivation of neurotropic simian immunodeficiency virus from exclusively lymphocytetropic parental virus: pathogenesis of infection in macaques. *J Virol* **66:** 3550–3556.

Somma-Mauvais H, Farnarier G (1992). Evoked potential in HIV infection. *Neurophysiol Clin* **22:** 369–384.

Takahashi K, Wesselingh SL, Griffin DE, McArthur JC, Johnson RT, Glass JD (1996). Localization of HIV-1 in human brain using polymerase chain reaction in situ hybridization and immunocytochemistry. *Ann Neurol* **39:** 705–711.

Weihe E, Nohr D, Sharer L, Murray E, Rausch D, Eiden L (1993). Cortical astrocytosis in juvenile rhesus monkeys infected with simian immunodeficiency virus. *NeuroReport* **4:** 263–266.

Westmoreland SV, Halpern E, Lackner A (1998). Simian immunodeficiency virus encephalitis in Rhesus Macaques is associated with rapid disease progression. *J NeuroVirol* **4:** 260–268.

Zhu GW, Liu ZQ, Joag SV, Pinson DM, Adany I, Narayan O, McClure HM, Stephens EB (1995). Pathogenesis of lymphocyte-tropic and macrophage-tropic SIV_{mac} infection in the brain. *J NeuroVirol* **1:** 78–91.